GEOPHYSICAL RESEARCH LETTERS, VOL. 14, NO. 8, PAGES 836-839, AUGUST 1987

M_m : THEORY OF A VARIABLE-PERIOD MANTLE MAGNITUDE

Emile A. Okal[1] and Jacques Talandier[2]

Abstract. We use classic expressions of the excitation and propagation of Rayleigh waves to develop a mantle magnitude M_m, measured at variable period between 40 and 300 s. We justify theoretically the use of distance and source excitation corrections, and obtain simplified expressions for them. We also explore the possible influence of the presence of a corner frequency in the spectrum. Finally, we relate frequency-domain measurements to the standard practice of measuring magnitudes in the time domain, and justify the latter for wavetrains with strong dispersion.

Introduction

The rapid measurement, if possible in real time and at a single seismic observatory, of the "size" of an earthquake remains an important aspect of observational Seismology; it motivated C.F. Richter's pioneering work, culminating in his introduction of the concept of magnitude [Richter, 1935]. Among the various magnitude scales later developed, the surface-wave magnitude M_s, obtained at a period close to 20 s, and standardized by the "Prague" formula [Vaněk et al., 1962], has become the most widely used measure of teleseismic events. Its popularity stems mainly from the abundance of 20-s Rayleigh wavetrains along oceanic paths, and the deployment, in the 1950s and 1960s, of instruments peaked precisely in this frequency range. Also, Geller and Kanamori [1977] showed that the modern-day M_s is basically equivalent to the older M, as used by Gutenberg and Richter [1954].

It has long been known, however, that any magnitude scale measured at a constant period T saturates when the duration of rupture along the fault becomes comparable to T. Thus for very large earthquakes, and in particular those carrying tsunami risk, M_s loses significance. On the other hand, the seismic moment M_0 introduced by Aki [1967], measured, at least in principle, at zero-frequency, keeps growing with earthquake size, rather than saturate. In addition, and because of the linearity of the laws of mechanics, the excitation of all seismic waves from an earthquake source is proportional to M_0.

About 20 years ago, Brune and King [1967] investigated the spectral amplitude of 100-s Rayleigh waves, but stopped short of fully defining a magnitude scale at this period. With the recent development of broadband seismographs providing adequate records of mantle Rayleigh waves even for relatively moderate earthquakes, it is now possible to envision their systematic use in the rapid estimation of the "size" of teleseismic events, in particular of their seismic moment. The purpose of this paper is to lay the theoretical grounds for the development of a magnitude scale M_m, measured on mantle Rayleigh waves, at a variable period (in practice $T \geq 40$ s), allowing the immediate estimation of the seismic moment of a distant earthquake. In a companion paper [Talandier et al., 1987; hereafter Paper 2], we give experimental results from the broadband station at Papeete, Tahiti, and describe briefly the automation of the method. In this endeavor, we are driven by two goals: first, retrieval of the seismic moment M_0, and second, retention of the concept of magnitude, with its direct relationship to the amplitude of ground motion. As a result, we define M_m as

$$M_m = \log_{10} M_0 - 20 \quad (1)$$

where M_0 is in dyn-cm. The constant 20 provides a simple link between M_m and M_0, and keeps M_m values in the general range of conventional magnitudes.

It should be noticed that in this fashion, we impose a slope of 1 between M_m and $\log_{10} M_0$. This differs from the case of M_w, for which Kanamori [1977] imposed a slope of 2/3, since he was specifically seeking to extend M_s to gigantic earthquakes, beyond its point of total saturation; as discussed in detail by Geller [1976], most "interesting" earthquakes (large, but not gigantic; typically $M_s = 7$) belong to a region where M_s has started to saturate, and grows only like $2/3 \log_{10} M_0$; hence the factor 2/3 in M_w. In our case, and for the purpose of retrieving M_0, it is easier and more natural to impose a slope of 1 between M_m and $\log_{10} M_0$. Finally, in this study, we restrict ourselves to shallow sources ($h \leq 75$ km), characteristic of large subduction zone events, and bearing substantial tsunami risk.

Theory

We base the development and measurement of M_m on the following theoretical approach [Kanamori and Stewart, 1976]. The spectral amplitude at angular frequency ω of a Rayleigh wave recorded at a distance Δ from an earthquake point source can be written:

$$X(\omega) = a \sqrt{\pi/2} \left[e^{-\omega a \Delta / 2UQ} / \sqrt{\sin\Delta} \right] \times \quad (2)$$

$$\times \left[\frac{1}{U} \left| s_R K_0 l^{-1/2} - p_R K_2 l^{3/2} - i q_R K_1 l^{1/2} \right| M_0 \right].$$

In this equation, we group separately terms due to propagation and excitation. The first line contains the geometrical spreading and the anelastic attenuation over the path $a\Delta$. The second line contains terms relating to excitation: the seismic moment M_0, and a combination of the excitation coefficients K_i (depending on depth and frequency), and of the trigonometric coefficients p_R, q_R, s_R, depending only on the particular geometry of faulting relative to the azimuth to the station. l is the angular order of the equivalent normal mode. We refer to Kanamori and Stewart [1976] for

[1]Department of Geological Sciences, Northwestern University, Evanston, Illinois 60201
[2]Laboratoire de Géophysique, C.E.A., Boîte Postale 640, Papeete, Tahiti

Paper number 7L7179.
0094-8276/87/007L-7179$03.00

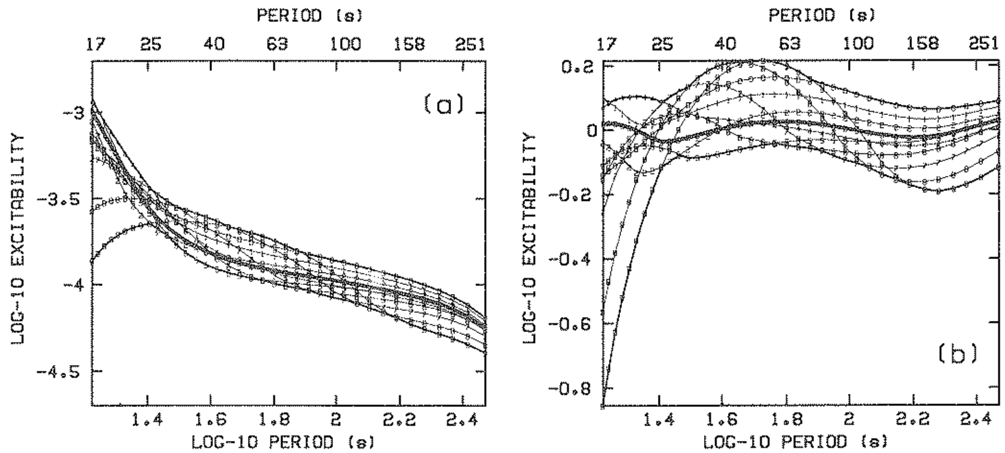

Fig. 1. Excitability of Rayleigh waves E_{av} as a function of depth and frequency. *(a):* Uncorrected data. Each line represents E_{av} at a given depth (between 10 km (symbol: 0) and 75 km (symbol: 9)), obtained by averaging the excitation over all possible focal geometries. The thicker trace is the value at 20 km. *(b):* Same as *(a)* after the correction given by Eqn. (4) has been applied. Note small deviation for $T > 40$ s.

the exact expression of these various coefficients. Conversely, this equation can be used to extract the seismic moment of the event through

$$\log_{10} M_0 = \log_{10} X(\omega) + C_D + C_S + C_0 \qquad (3)$$

where C_D is a distance correction, C_S a source correction, and $C_0 = \log_{10}(\sqrt{(2/\pi)}/a) = -3.90$ a constant. Eqn. (3) lays the ground for the definition of a magnitude scale at variable frequency.

Distance Correction C_D

This correction is simply $C_D = 0.5 \log_{10} \sin\Delta + (\log_{10} e)\, \omega a\, \Delta / 2UQ$. These terms are independent of focal geometry and depth; given a model of dispersion and attenuation for a particular path, C_D is readily computed and can be catalogued as a function of distance and frequency alone. In practice, and for the dataset described in Paper 2, we use a regionalized model of the Pacific Ocean, with dispersion and attenuation based on the models of Canas and Mitchell [1978], Mitchell and Yu [1980] and Nakanishi [1981]. The path under study is then split into segments of various ages, and their contributions to C_D added.

Source Correction C_S

This correction is $C_S = -\log_{10} \left| \left(s_R K_0 l^{-1/2} - p_R K_2 l^{3/2} - i\, q_R K_1 l^{1/2} \right) / U \right|$. It is somewhat more complex and depends on a combination of frequency, depth, and focal geometry. For the purpose of obtaining rapidly, in real time, an earthquake magnitude (by definition an order of magnitude of the size of the earthquake), it is legitimate to assume that the focal geometry of the event is unknown, and to use a correction averaged over the orientation of the focal mechanism. Figure 1*a*, shows values of the "excitability" E_{av} as a function of period and depth (10 km $\leq h \leq$ 75 km), in the PREM model, obtained by averaging the second bracket in (2) over a set of 3240 focal geometries. Using E_{av} instead of the exact excitation results in a systematic error for an event with "pure" focal geometry (either horizontal or vertical slip on a perfectly vertical fault plane), and a station at the node of the radiation pattern. For other mechanisms, in particular the thrust faults characteristic of the catastrophic events at subduction zones, it is general possible to find a period at which the sharpness of the nodes of the radiation pattern is considerably reduced (see example below); under these conditions, the error usually remains less than $\pm$ 0.2 unit of magnitude. It is clear from Figure 1*a* that the dependence of E_{av} on depth is minimal for periods $T \geq 40$ s. If C_S is modeled by the cubic spline best-fitting E_{av} (20 km):

$$C_S = 2.0398\, \theta^3 - 1.3122\, \theta^2 + 0.39342\, \theta + 3.9335 \qquad (4)$$

where $\theta = \log_{10} T - 1.7657$, Figure 1*b* shows that the deviation of E_{av} is at most ± 0.2 order of magnitude between the depths of 10 and 75 km. The range of variation of C_S itself is only 3.92 ± 0.2 between 40 and 150 s, when M_0 is in units of 10^{27} dyn-cm. Eqns. (1) and (3) then yield:

$$M_m = \log_{10} X(\omega) + C_D + C_S - 0.90 \qquad (5)$$

where $X(\omega)$ is in μm-s.

Influence of Source Duration; Correction C_{CF}.

For most earthquakes with moments in the 10^{27} to 10^{28} dyn-cm range, one expects the first corner frequency due to finite length of rupture to occur in the 8 to 20 mHz second range [Geller, 1976]. As a result, and for the larger events, some measurements taken in the 40 to 150 s period range are expected to fall beyond the corner frequency ω_{CF}, and thus require a correction due to source duration. This need could be alleviated by using waves of even longer periods. As discussed below, we prefer using a range of magnitudes for the determination of M_m, to guard against possible focal geometry artifacts.

Source duration interferes with the amplitude spectrum $X(\omega)$ through an additional factor sinc $(\omega \tau_s / 2)$, where τ_s is the source duration. Conversely, beyond ω_{CF}, this warrants an additional correction

$$C_{CF} = \log_{10}(\pi\, \tau_s \,/\, T) \qquad (6)$$

to M_m in (5), since the sine function in 'sinc' approaches 1 beyond ω_{CF}.

In principle, if major earthquakes follow scaling laws with constant stress drop $\Delta\sigma$, one expects the length of rupture, and consequently τ_s, to grow as $M_0^{1/3}$ [Kanamori and Anderson, 1975]. For $\Delta\sigma =$ 50 bar, Geller [1976] obtains $\tau_s = 18\, M_0^{1/3}$, where τ_s is in seconds and M_0 in units of 10^{27} dyn-cm. Eqn. (5) then becomes

$$M_m = 1.5\,[\,\log(X(\omega)\,/T\,) + C_S + C_D\,] - 2.22 \qquad (7)$$

In practice, the systematic inversion of source parameters of moderate to large earthquakes [e.g., Dziewonski and Woodhouse, 1983] confirms the growth of τ_s with M_0, but with considerable scatter, and generally somewhat slower than $M_0^{1/3}$. Indeed, for the dataset used in Paper 2, a logarithmic regression of published values of τ_s (or L) versus M_0 yields a slope of only 0.09, with a linear correlation coefficient of only 0.045, suggesting poor scaling of τ_s with M_0.

Several reasons may exist for this violation of scaling laws: the geometry of rupture may be variable, involving bi-directional faults; the velocity of rupture is known to vary substantially, and the stress drop itself could vary; more significantly, heterogeneity along the fault zone, in the form of asperities [Lay and Kanamori, 1981] or barriers [Aki, 1979], can lead to jerky stress release, poorly described by a constant rupture velocity (however, the finiteness of the rupture velocity remains a valid concept, and catastrophic earthquakes in the 10^{29} to 10^{30} dyn-cm range are known to have significantly longer durations).

In view of these results, we also consider a model with constant $\tau_s = 35$ s (this is the average value for the dataset in Paper 2), and obtain a corner frequency correction $C_{CF} = 2.04 - \log_{10}T$. Eqn. (7) is then replaced by

$$M_m = \log_{10}[\,X(\omega)\,/\,T\,] + C_S + C_D + 1.14 \qquad (8)$$

Time-Domain Measurements

The above theory was developed in the frequency domain, and makes use of the spectral amplitude $X(\omega)$. In order to relate M_m more closely to standard magnitudes measured in the time domain, we explore in this section the relationship between the time-domain seismic amplitude $x(t)$ and $X(\omega)$.

The mantle waves used for the measurement of M_m are strongly (and inversely) dispersed between 40 and about 300 s, and a typical Rayleigh seismogram (once the higher frequencies have been filtered out) can be approximated by a succession of sinusoid arches (or half-periods) of increasing periods and generally decreasing amplitudes. The spectral amplitude of a signal $x(t)$ consisting of a single, complete period of a sinusoid of angular frequency ω_0, and zero-to-peak amplitude a_0 can be written, in the vicinity of $\omega = \omega_0$:

$$X(\omega) = \frac{1}{2}\, a_0\, T_0\, \mathrm{sinc}[\frac{1}{2}(\omega_0 - \omega)T_0] \qquad (9)$$

(we have simply neglected a term substantial only for negative ω). If the dispersion of the signal is strong, i.e., if the approximate period of each oscillation of the signal is sufficiently distant from the previous one, the spectrum of each arch should not be affected too much by the side lobes of the other sinc functions, and

$$X(\omega_0) \approx a_0\, T_0\,/\,2 \qquad (10)$$

Although this approximation is extremely crude, it works surprisingly well, as demonstrated by the example on Figure 2*a*: we consider a synthetic time series consisting of 5 arches of periods ranging between 40 and 200 seconds and with amplitudes decreasing from 1 to 0.45 cm. Figure 2*b* shows the spectrum of this signal (solid curve) and compares it to measurements made in the time domain using (10). The deviation between the two methods is only -0.05±0.08 units of magnitude. This result, also upheld experimentally by the dataset in Paper 2, gives some theoretical basis to the 50-yr old practice of using time-domain measurements in the computation of seismic magnitudes.

The above remark leads to the following formulæ for direct measurement of M_m in the time domain:

$$M_m = \log_{10}(a \cdot T) + C_D + C_S - 1.20 \qquad (11a)$$

(flat spectrum),

$$M_m = 1.5\,[\,\log_{10} a_0 + C_S + C_D\,] + 3.18 \qquad (11b)$$

($\tau_s \sim M_0^{1/3}$ scaling), and

$$M_m = \log_{10} a_0 + C_S + C_D + 0.84 \qquad (11c)$$

(constant τ_s).

Why a Variable Period ?

Finally, we justify the concept of using a variable period to determine M_m. It would seem *a priori* more rational to use a constant period for easier reference; this is indeed common practice for other magnitude

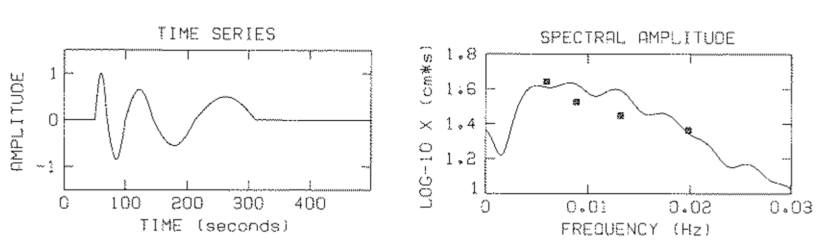

Fig. 2. Approximation to Rayleigh wavetrain made of five sinusoid arches of decreasing frequencies and amplitudes. *Left:* Time series. *Right:* Spectral domain; the solid symbols are obtained from Eqn. (9), the solid line from a rigorous FFT.

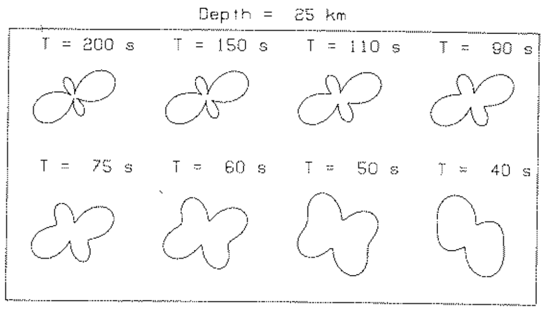

Fig. 3. Azimuthal radiation patterns of the spectral amplitude X for various periods, in the geometry $\phi = 13°$; $\delta = 71°$; $\lambda = 36°$. Note disappearance of secondary nodes at higher frequencies.

scales. However, we want to guard against the possibility of a station sitting in a node of Rayleigh wave radiation at a particular period. Obviously, in the case of a "pure" geometry such as a strike-slip earthquake on a vertical fault, the azimuth of the nodes are frequency-independent; however, as shown on Figure 3, the shape of radiation patterns can be extremely dependent on frequency for focal geometries involving non-vertical faults and/or oblique slip. A change of reference period can literally move the station out the node. Similarly, source finiteness can result in strong spectral holes beyond the corner frequency. By computing M_m at various periods, and retaining its maximum value, one can hope to eliminate such problems, and more precisely estimate the earthquake's moment.

Conclusion

We have shown that surface wave theory predicts the simple Eqn. (5) relating M_m as defined by Eqn. (1) and the spectral amplitude of a low-frequency Rayleigh wave. We have obtained expressions of the necessary corrections C_D and C_S. We also discuss the possible influence of cornered spectra on such measurements, which would lead to Eqns. (7) or (8). Furthermore, we have shown that the common measurement of magnitudes in the time domain can be justified, at least for very-low frequencies. The present paper thus sets the stage for routine and automatic measurements of M_m; we show in Paper 2 that Eqns. (5) and (11a), give an excellent fit to a variety of datasets.

Acknowledgments. We thank Seth Stein and Otto Nuttli for comments. This research was supported by Commissariat à l'Energie Atomique, and the National Science Foundation under Grant EAR-84-05040.

References

Aki, K., Scaling law of seismic spectrum, *J. Geophys. Res., 72,* 1217-1231, 1967.

Aki, K., Characterization of barriers on an earthquake fault, *J. Geophys. Res., 84,* 6140-6148, 1979.

Brune, J.N., and C.-Y. King, Excitation of mantle Rayleigh waves of period 100 s as a function of magnitude, *Bull. Seism. Soc. Am., 57,* 1355-1365, 1967.

Canas, J.A., and B.J. Mitchell, Lateral variation of surface-wave anelastic attenuation across the Pacific, *Bull. Seism. Soc. Am., 68,* 1637-1650, 1978.

Dziewonski, A.M., and J.H. Woodhouse, An experiment in systematic study of global seismicity: Centroid-moment tensor solutions for 201 moderate and large earthquakes in 1981, *J. Geophys. Res., 88,* 3247-3271, 1983.

Geller, R.J., Scaling relations for earthquake source parameters and magnitudes, *Bull. Seism. Soc. Am., 66,* 1501-1523, 1976.

Geller, R.J., and H. Kanamori, Magnitudes of great shallow earthquakes from 1904 to 1952, *Bull. Seism. Soc. Am., 67,* 587-598, 1977.

Gutenberg, B., and C.F. Richter, *Seismicity of the Earth and associated phenomena,* 310 pp., Princeton Univ. Press, Princeton, N.J., 1954.

Kanamori, H., The energy release in great earthquakes, *J. Geophys. Res., 82,* 2981-2987, 1977.

Kanamori, H., and D.L. Anderson, Theoretical basis of some empirical relations in seismology, *Bull. Seism. Soc. Am., 65,* 1073-1095, 1975.

Kanamori, H., and G.S. Stewart, Mode of strain release along the Gibbs Fracture Zone, Mid-Atlantic Ridge, *Phys. Earth Planet. Inter., 11,* 312-332, 1976.

Lay, T., and H. Kanamori, An asperity model of great earthquake sequences, *in: Earthquake prediction, an international review,* edited by D.W. Simpson and P.G. Richards, *Maurice Ewing Ser., 4,* pp. 579-592, AGU, Washington, D.C., 1981.

Mitchell, B.J., and G.-K. Yu, Surface-wave dispersion, regionalized velocity models, and anisotropy of the Pacific crust and upper mantle, *Geoph. J. R. astr. Soc., 63,* 497-514, 1980.

Nakanishi, I., Shear velocity and shear attenuation models inverted from the world-wide and pure-path average data of mantle Rayleigh waves (${}_0S_{25}$ to ${}_0S_{80}$) and fundamental spheroidal modes (${}_0S_2$ to ${}_0S_{24}$), *Geoph. J. R. astr. Soc., 66,* 83-130, 1981.

Richter, C.F., An instrumental earthquake magnitude scale, *Bull. Seism. Soc. Am., 25,* 1-32, 1935.

Talandier, J., D. Reymond, and E.A. Okal, M_m: Use of a variable-period mantle magnitude for the rapid one-station estimation of teleseismic moments, *Geophys. Res. Letts., 14,* this issue, 1987.

Vaněk, J., A. Zátopek, V. Kárník, N.V. Kondorskaya, Yu. V. Riznichenko, E.F. Savarenskii, S.L. Solov'ev, and N.V. Shebalin, Standardization of magnitude scales, *Izv. Akad. Nauk SSSR, Ser. Geofiz., 2,* 153-158, 1962.

(Received May 18, 1987;
accepted June 5, 1987.)